

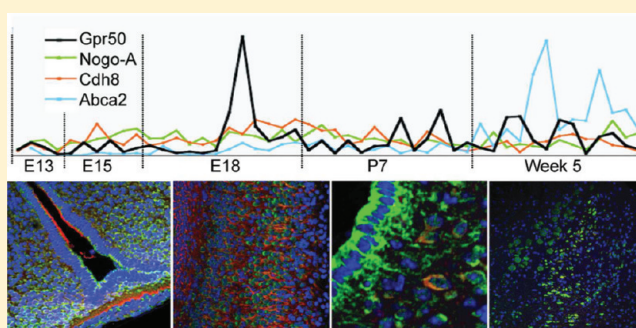
## Developmental Expression of Orphan G Protein-Coupled Receptor 50 in the Mouse Brain

Ellen Grünewald,<sup>†</sup> Kenneth D. Tew,<sup>‡</sup> David J. Porteous,<sup>†</sup> and Pippa A. Thomson<sup>\*†</sup><sup>†</sup>Medical Genetics Section, The University of Edinburgh, Institute of Genetics and Molecular Medicine, Molecular Medicine Centre, Crewe Road, Edinburgh EH2 4XU, United Kingdom<sup>‡</sup>Department of Cell and Molecular Pharmacology and Experimental Therapeutics, Medical University of South Carolina, Charleston, South Carolina 29425, United States

## Supporting Information

**ABSTRACT:** Mental disorders have a complex etiology resulting from interactions between multiple genetic risk factors and stressful life events. Orphan G protein-coupled receptor 50 (GPR50) has been identified as a genetic risk factor for bipolar disorder and major depression in women, and there is additional genetic and functional evidence linking GPR50 to neurite outgrowth, lipid metabolism, and adaptive thermogenesis and torpor. However, in the absence of a ligand, a specific function has not been identified. Adult GPR50 expression has previously been reported in brain regions controlling the HPA axis, but its developmental expression is unknown. In this study, we performed extensive expression analysis of GPR50 and three protein interactors using rt-PCR and immunohistochemistry in the developing and adult mouse brain. Gpr50 is expressed at embryonic day 13 (E13), peaks at E18, and is predominantly expressed by neurons. Additionally we identified novel regions of Gpr50 expression, including brain stem nuclei involved in neurotransmitter signaling: the locus coeruleus, substantia nigra, and raphe nuclei, as well as nuclei involved in metabolic homeostasis. Gpr50 colocalizes with yeast-two-hybrid interactors Nogo-A, Abca2, and Cdh8 in the hypothalamus, amygdala, cortex, and selected brain stem nuclei at E18 and in the adult. With this study, we identify a link between GPR50 and neurotransmitter signaling and strengthen a likely role in stress response and energy homeostasis.

**KEYWORDS:** GPR50, Nogo-A, Cadherin 8, ABCA2, rt-PCR, immunohistochemistry



Psychiatric disorders are a major health problem in the world today. One in four people are affected by mental disorders during their lives, according to the World Health Organization.<sup>1</sup> Psychiatric illness results from the interaction between genetic and environmental risk factors. There is a strong genetic component, as is clear from family, twin, and adoption studies.<sup>2</sup> Recently, G protein-coupled receptor 50 (GPR50) was identified as a risk gene for bipolar disorder and major depression in Scottish women.<sup>3,4</sup> GPR50, previously known as the melatonin-related receptor, is the mammalian ortholog of the melatonin 1c receptor (Mel1c).<sup>5</sup> Despite a 45% sequence identity to melatonin receptors MT1 and MT2, it does not bind melatonin or any other ligand and therefore remains an orphan receptor without a clear function.<sup>6,7</sup> We have recently reported the results of a yeast two-hybrid study (Y2H), identifying interactors with the relatively large GPR50 C-terminal domain.<sup>8</sup> Interactors can be grouped into two functional classes by gene ontology: neural development and sterol metabolism, indicating a likely role in these mechanisms. In addition, we showed that GPR50 has a dramatic effect on the neurite outgrowth, supporting a likely role in neural development.<sup>8</sup> Although the list of interactors includes several interesting protein partners,

we know little about where and when these proteins could interact and what function the interactions would have.

Functional evidence for a link to lipid metabolism is indicated by the association of GPR50 sequence variants with elevated triglycerides and lower circulating HDL-cholesterol levels,<sup>9</sup> and Gpr50 knockout mice show hyperactivity, higher metabolic rates, and resistance to obesity when fed on a high energy diet.<sup>10</sup> A recent study identified a role for GPR50 in adaptive thermogenesis and torpor,<sup>11</sup> the body's response to food shortage. The absence of Gpr50 resulted in a rapid onset of torpor in mice and was associated with a diminished responsiveness to leptin, and a reduction in the expression of hypothalamic thyrotropin-releasing hormone (TRH). Additionally, there appears to be a function for GPR50 in modifying MT receptor signaling. The receptors are shown to heterodimerize and GPR50 can also inhibit MT1 signaling via its intracellular C-terminal domain.<sup>12</sup>

Received: January 19, 2012

Accepted: April 14, 2012

Published: April 15, 2012

GPR50 expression has previously been found in the hypothalamus, the pituitary, and the adrenal, in humans, rodents, and sheep, suggesting a role in the HPA axis and neuroendocrine system.<sup>13–15</sup> GPR50 is thought to be expressed by tanycytes, a glial cell type lining ependyma of the third ventricle, in a seasonal pattern.<sup>16</sup> Nothing is known however about its developmental expression.

In order to investigate the spatial and temporal expression patterns of GPR50 and its interactors as identified by Y2H, we performed rt-PCR and immunohistochemistry in the developing and adult mouse brain. We have previously confirmed the interaction of neurite outgrowth inhibitor Nogo-A with GPR50.<sup>8</sup> Here we choose to also investigate the interaction with and coexpression of Y2H interactors calcium-dependent cell–cell adhesion molecule cadherin 8 (CDH8) and the ATP-binding cassette transporter-2 (ABCA2), because of the known involvement of CDH8 and other cadherins in brain development<sup>17</sup> and a role of ABCA2 in maintaining homeostasis of cholesterol, steroids, and lipids.<sup>18,19</sup> rt-PCR on 48 regional samples at developmental stages E13, E15, E18, day 7, and week 5 was followed up by immunohistochemistry in the E18 and adult mouse brain using protein-specific antibodies and markers.

## RESULTS AND DISCUSSION

### Subcellular Localization of GPR50, CDH8, and ABCA2.

To investigate where GPR50 is coexpressed with CDH8 and ABCA2, immunocytochemistry and subcellular fractionation experiments were performed. In addition, coimmunoprecipitations were performed to investigate whether GPR50 interacts with CDH8 and ABCA2 under overexpressed conditions. In neuroblastoma cells, overexpressed GPR50 colocalizes with exogenous ABCA2 in the endosomal and lysosomal compartments and with exogenous CDH8 in the plasma membrane (Figure 1A). Coimmunoprecipitations in HEK293T cells show that overexpressed ABCA2 and CDH8 coprecipitate with GPR50 (Figure 1B). Subcellular fractionation experiments of adult mouse brain have previously shown endogenous expression and enrichment of Gpr50 and Nogo-A in the pre- and postsynaptic density fractions. These proteins are also present, but less enriched, in the crude synaptosome (P2) and light membrane (P3, includes ER, golgi, endolysosome) fractions.<sup>8</sup> In a similar experiment, Cdh8 and Abca2 were both detected in the light membrane, crude synaptosome, and synaptosomal fraction (Figure 1C). Gpr50 does not appear to be expressed in myelin, as is known for Nogo-A,<sup>20</sup> suggesting it is not expressed by oligodendrocytes.

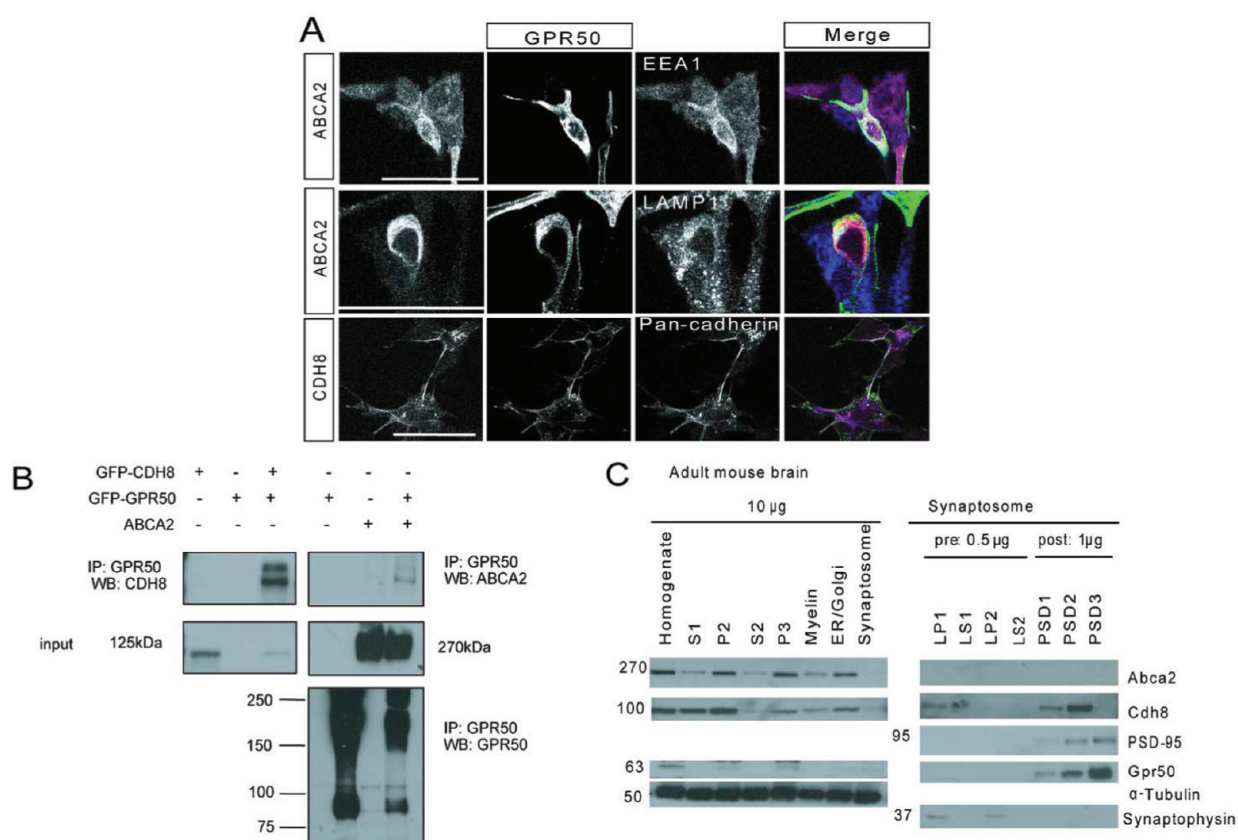


**Figure 1.** Interactions and subcellular localization of GPR50, CDH8, and ABCA2. (A) SH-SY5Y cells were cotransfected with GPR50 and ABCA2 or CDH8 and costained with endosomal marker EEA1, lysosomal marker LAMP1, or plasma membrane marker pan-cadherin. GPR50 colocalizes with ABCA2 in the endosome and lysosome and with CDH8 on the cell membrane. Scale bars: 50 µm. (B) HEK293T cells were cotransfected with GPR50, CDH8, ABCA2 or cotransfected with GPR50 and ABCA2. Lysates were immunoprecipitated with GPR50 antibody. Western blots were probed with CDH8 or ABCA2 revealing coimmunoprecipitations of both proteins with GPR50. (C) Western blot after subcellular fractionation of 10 adult female mouse brains. CDH8 is enriched in the presynaptic membrane fraction (LP1) and in the postsynaptic PSD1 and PSD2 fractions. ABCA2 is expressed in low levels in the synaptosome but not detected in the specific synaptosomal fractions. Pre- and postsynaptic fractions are marked by expression of synaptophysin and PSD-95.

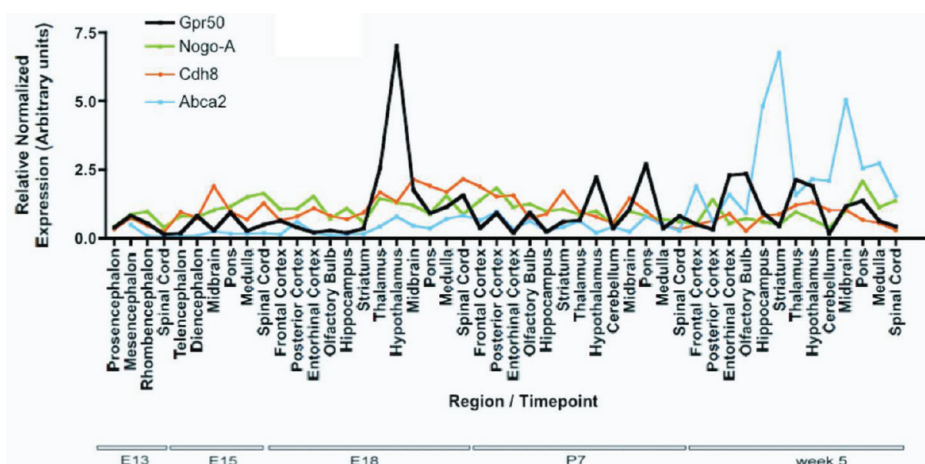


**Figure 2.** Real-time quantitative rt-PCR on Origene mouse developmental panel with 48 regional brain samples from five developmental stages. Relative normalized expression values of *Gpr50*, *Nogo-A*, *Nogo-C*, *Cdh8* and *Abca2* normalized to  $\beta$ -Actin, *Tbp*, *Hmbs*, and cyclophilin B.

*Cdh8* was found to be enriched in the presynaptic membrane fraction and in the postsynaptic density fractions (Figure 1C), in line with its previously detected localization at synaptic junctions and suggested role in cell–cell adhesion at synaptic contacts.<sup>21</sup> ABCA2 was reported to localize to intracellular lysosomal fractions, but may also relocate to other cell membrane compartments.<sup>19</sup> This indicates GPR50, CDH8, and ABCA2 may be interaction partners at the synapse or in internal membranes.

**Developmental Expression of *Gpr50* and Interactors by rt-PCR.** To determine where and when *GPR50* is expressed and available to interact with its partners, rt-PCR was performed on a developmental mouse brain panel (Origene) covering 48 regional samples over five time points, E13, E15, E18, P7, and week 5. Data was normalized against four housekeeping genes ( $\beta$ -actin, *Tbp*, *Hmbs*, and *cyclophilin*) with varying levels of expression (Ct value, Supporting Information Table 1) to reflect the difference in expression levels between our genes-of-interest (Supporting Information Table 1).

Relative normalized expression of *Gpr50*, *Nogo-A*, *Cdh8*, and *Abca2* is shown in Figure 2. *Gpr50* mRNA was detected in low levels from E13, peaked at E18, and increased again at week 5. At most developmental time points, *Gpr50* shows a restricted expression pattern with highest expression in thalamus, in hypothalamus (diencephalon), and in the midbrain, pons, and medulla (mesencephalon, rhombencephalon). *Nogo-A* mRNA expression is extensive and constant and was detected throughout all regions and time points. *Cdh8* expression is relatively constant but did show an increase in the posterior regions at E18 and frontal regions at day 7. *Abca2* expression is lower during early development and increases at week 5. The results suggest an increased expression of the genes around E18 and/or at 5 weeks, indicating possible coregulation.

To test this Spearman correlations ( $r$ ) were performed of the overall data (between the genes for all regions and ages, using the above genes plus *Nogo-pan* (detecting *Nogo-A-B*, and *-C*), *Gpr50* correlates significantly with *Abca2* (Spearman's  $r$  (95% confidence interval);  $p$ -value): ( $r = 0.43$  (0.15–0.64);  $p = 0.0028$ ). Other significant correlations are *Nogo-pan* with *Cdh8* ( $r = 0.39$  (0.11–0.61);  $p = 0.0068$ ), *Nogo-pan* with *Abca2* ( $r = 0.40$  (0.12–0.62);  $p = 0.0058$ ), and *Nogo-A* with *Cdh8* ( $r = 0.32$  (0.03–0.56);  $p = 0.0268$ ). As expected, *Nogo-pan* correlates with *Nogo-A* ( $r = 0.37$  (0.09–0.60);  $p = 0.0097$ ).

Because *Gpr50* shows increased expression around E18, Spearman correlations were calculated for age E18 only. At this

time point, *Gpr50* correlates significantly with *Cdh8* ( $r = 0.64$  (0.09–0.89);  $p = 0.024$ ) and again with *Abca2* ( $r = 0.71$  (0.20–0.91);  $p = 0.0102$ ). Other significant correlations were found between *Nogo-pan* and *Abca2* ( $r = 0.71$  (0.20–0.91);  $p = 0.0102$ ) and between *Cdh8* and *Abca2* ( $r = 0.68$  (0.15–0.90);  $p = 0.0153$ ). By contrast, no significant correlations were found at week 5. These results may indicate possible coregulation between *GPR50* and *ABCA2* overall and *CDH8* at E18 only.

#### ***Gpr50* Is Expressed in Hypothalamic and Brainstem Nuclei.**

Subregional expression and coexpression of our proteins of interest at the cellular level was investigated by immunohistochemistry in mouse brain at E18, when *Gpr50* was found to be most highly expressed, and in the adult. In accordance with the rt-PCR results, the coronal planes containing the hypothalamus and third ventricle, the midbrain, pons, medulla, and cerebellum were investigated (see Methods for details). Both chromogenic and fluorescent detection methods were used. Control experiments show absence of signal using a *GPR50* blocking peptide, indicating specific staining of the antibody (Supporting Information Figure 1A). The relative normalized expression levels of *Gpr50* mRNA as measured by rt-PCR and levels of protein expression as detected by immunohistochemistry in E18 and adult mouse brain are summarized in Table 1. In agreement with previous reports<sup>14</sup> and with the rt-PCR data, *Gpr50* is highly expressed in the hypothalamus around the third ventricle, the amygdala, amygdalar or piriform cortex, and the entorhinal and somatosensory cortices. Hippocampal expression of *Gpr50* was detected on the midbrain level in the adult brain only, in the polymorph layer of the dentate gyrus, which is the primary target for noradrenergic, serotonergic, and cholinergic input to the hippocampus.<sup>22</sup> At the midbrain level, *Gpr50* is also expressed in the cortex and in agreement with the rt-PCR data the ventral pons. *Gpr50* appeared to be moderately expressed in the ventral midbrain, in the substantia nigra pars compacta. In more posterior regions in the brain, *Gpr50* expression is found at low levels in the midbrain and pontine raphe nuclei, the cortex, and the superior colliculus. In the pons and medulla, *Gpr50* is moderate to highly expressed in several brainstem nuclei, including strong expression in the locus coeruleus. *Gpr50* expression is also found in the inferior colliculus and in low levels in the Purkinje cell layer of the cerebellum (Table 1). There was much agreement in protein expression levels as detected by chromogenic and fluorescent methods except for

Table 1. Expression Levels of Gpr50 in the Mouse Brain<sup>a</sup>

region	Gpr50 mRNA	Gpr50 protein	Nogo-A	Cdh8	Abca2	region	Gpr50 mRNA	Gpr50 protein	Nogo-A	Cdh8	Abca2
E18						week 5/10					
frontal cortex	0.637	+++	Y	Y	N	subparaventricular zone		++	Y	N	N
posterior cortex	0.394	+++	Y	Y	N	ependyma of third ventricle		+++	N	N	Y
entorhinal cortex	0.202	×	×	×	×	dorsomedial hypothalamus		++	Y	N	N
olfactory bulb	0.285	×	×	×	×	ventromedial hypothalamus		++	N	Y	Y
hippocampus	0.198	-	N	N	N	lateral hypothalamus		+	Y	N	N
striatum	0.36	-	N	N	N	arcuate nucleus		++	Y	N	Y
thalamus	2.57	++	N	N	N	median eminence		++	N	N	Y
hypothalamus	7.015	+++	N	Y	N	cerebellum	0.169				
midbrain	1.768	+	N	N	N	Purkinje cell layer		+	N	N	N
pons	0.906	+	Y	Y	N	cerebellum other		-	N	N	N
medulla	1.138	++	Y	Y	N	midbrain	1.163				
spinal cord	1.559	×	×	×	×	superior colliculus		++	Y	N	Y
week 5/10						periaqueductal gray		+	N	N	N
frontal cortex	0.51	×	×	×	×	substantia nigra		+/++	N	N	N
posterior cortex	0.323	×	×	×	×	pons	1.364				
motor cortex		+	Y	N	Y	raphe nuclei		+	N	N	N
somatosensory cortex		++	Y	N	Y	locus coeruleus		+++	N	N	Y
visual cortex		++	Y	N	Y	mesencephalic trigeminal nucleus		+	Y	Y	Y
entorhinal cortex	2.306	++	Y	N	Y	pontine gray		++	N	N	N
piriform cortex		++	Y	N	Y	medulla	0.635				
olfactory bulb	2.352	×	×	×	×	inferior colliculus		++	Y	N	Y
hippocampus	0.939					gigantocellular reticular nucleus		++	N	N	Y
dentate gyrus medial blade polymorph layer		+	N	N	N	magnocellular reticular nucleus		++	N	N	Y
hippocampus other		-	N	N	N	parvocellular reticular nucleus		++	N	N	Y
amygdala		++	Y	Y	Y	principal sensory nucleus of the trigeminal		++	N	N	Y
striatum	0.445	-	N	N	N	spinal cord	0.433	×	×	×	×
thalamus	2.134	++	N	N	N						
hypothalamus	1.906										
suprachiasmatic nucleus		++	N	N	N						

<sup>a</sup>Column 1: Relative normalized Gpr50 mRNA expression levels as measured by rt-PCR at E18 and week 5. Column 2: Semiquantitative evaluation of Gpr50 protein expression after immunohistochemistry at E18 and the Week 10. Scale: ×, not investigated; -, no expression present; +, weak expression; ++, moderate expression; +++, strong expression. Columns 3–5: Colocalization of Gpr50 and Nogo-A, Cdh8 or Abca2 as measured by immunohistochemistry. Scale: ×, not investigated; Y, colocalisation detected; N, no colocalization detected.

the substantia nigra, which showed clearer Gpr50 expression when using a HRP secondary and DAB than when using fluorescent secondary antibodies (Supporting Information Figure 2). This perhaps reflects the greater sensitivity of the DAB method.<sup>23</sup>

**Gpr50 Expression in Neurons.** Few studies have investigated the specific cell type(s) that express GPR50. In the ependyma of the third ventricle, Gpr50 is thought to be expressed by tanycytes as determined by location, morphology, and colabeling with vimentin or Glut1,<sup>11,16,24</sup> and by neurons in the dorsomedial hypothalamus.<sup>24</sup> As we identified novel regions of Gpr50 expression, we carried out immunofluorescence colocalization of Gpr50 with cell type markers NeuN (mature neurons), GFAP (astrocytes), and O4 (oligodendrocytes). Gpr50 colocalizes with NeuN the cortex, midbrain, superior colliculus, pons, hippocampus, and brain stem nuclei (Figure 3A–J). In the locus coeruleus, colocalization between Gpr50 and NeuN was not as clear (Figure 3J) but weak NeuN staining in locus coeruleus neurons has been reported previously.<sup>25</sup> Gpr50 does not colocalize with GFAP, O4, or vimentin in any of these regions (not shown). The increased expression of Gpr50 at embryonic stages also suggests a predominant expression by neurons.

**Gpr50 Expression in Monoaminergic Neurons.** The apparent expression of Gpr50 in several brain stem nuclei of

behavioral importance is intriguing and was further investigated by colabeling of Gpr50 with 5-HT (serotonergic marker), tyrosine hydroxylase (TH, dopaminergic and noradrenergic marker), and dopamine beta hydroxylase (DBH, noradrenergic neuronal marker) in the adult mouse brain (Figure 4A–E). The strongest Gpr50 expression was detected in the locus coeruleus, where clear colocalization with DBH was detected (Figure 4A). Gpr50 is only expressed in low levels in the nucleus raphe magnus where it colocalizes with 5-HT (Figure 4B). Other areas of 5-HT expression including the pontine gray and the substantia nigra also showed colocalization with Gpr50 (Figure 4C, D). Gpr50 staining by immunofluorescence was weaker in the substantia nigra than with DAB (Table 1, Supporting Information Figure 2). Colocalization with 5-HT (Figure 4D) and TH (Figure 4E) in this area was therefore present but not strong.<sup>22</sup> These brain stem nuclei are highly interconnected with other areas in the brain, including the hypothalamus,<sup>26</sup> and the neuromodulatory and behavioral properties of the monoaminergic neurotransmitters have been well researched. Dopamine plays a role in movement, reward, and addiction; serotonin is implicated in appetite, mood, and anxiety; and noradrenaline is involved in fight-or-flight reaction, stress, and depression. In the absence of a ligand for Gpr50, its expression in the brainstem and colocalization with noradrenergic, dopaminergic, and serotonergic markers is

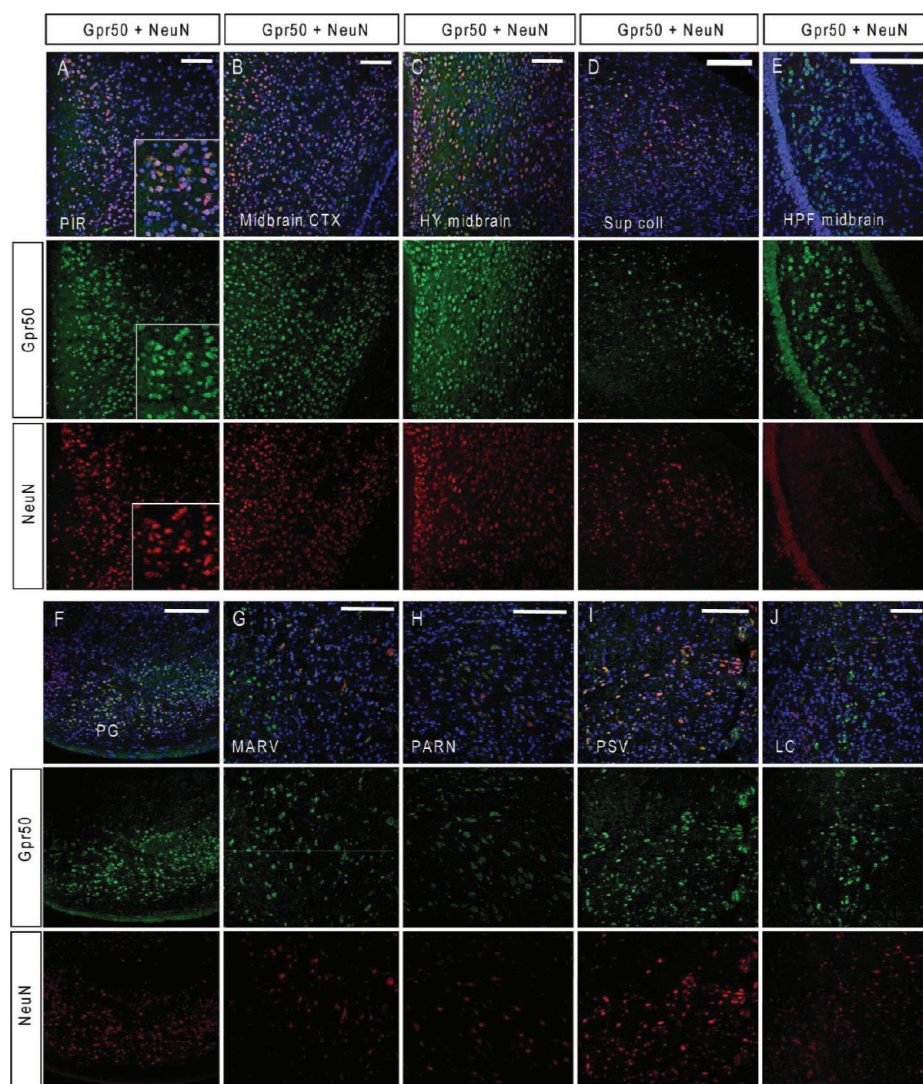


**Figure 3.** Colabeling of Gpr50 and NeuN in the adult mouse brain. CD1 brains were fixed in 70% EtOH and stained for Gpr50 and NeuN (A–E). PIR = piriform cortex, CTX = cortex, HY = hypothalamus, Sup coll = superior colliculus, HPF = hippocampal formation, PG = pontine gray, MARV = magnocellular reticular nucleus, PARN = parvocellular reticular nucleus, PSV = principal sensory nucleus of the trigeminal, LC = locus coeruleus. Sections were counterstained with DAPI. Scale bar: 100  $\mu$ m.

intriguing and introduces the possibility that Gpr50 is a receptor for these neurotransmitters, or that Gpr50 is involved in the regulation of monoamine transmission. Given its localization along the HPA axis, a neuropeptide ligand may also be possible. Using different antibodies and conditions, Gpr50 expression has also recently been reported in the dorsomedial nucleus of the hypothalamus and median eminence of male adult rodent, sheep, and human brain.<sup>11,24,27</sup> In rodents, Gpr50 expression was also found in the lateral hypothalamic area, periventricular nucleus, and amygdala.<sup>11,24,27</sup> In these studies, Gpr50 appears to be expressed mainly in the fibers which may be due to the differences in antibodies, methods, and sex of animals used.

#### Gpr50 Colocalization with Nogo-A, Abca2, and Cdh8.

Next we investigated whether Gpr50 colocalized with its interactors in the E18 and adult mouse brain. The expression of Nogo-A, Abca2, and Cdh8 was in agreement with previous studies.<sup>28–31</sup> In addition, control experiments show absence of signal in secondary antibody only controls, indicating specificity of the antibodies used (Supporting Information Figure 1B). In

the adult mouse brain, colocalization of Gpr50 and Nogo-A was found in several areas in the hypothalamus: the subparaventricular zone (Figure 5A and inset), arcuate nucleus/ventromedial hypothalamus (Figure 5B and inset), dorsomedial hypothalamus (Figure 5C and inset), and lateral hypothalamus (Figure 5D and inset). In each of these areas it appears to be a small subset of cells that express both. Colocalization of Gpr50 and Nogo-A is more widespread in the amygdala (Figure 5E and inset), and is also found in the superior colliculus (Figure 5F and inset) and the somatosensory cortex (Figure 5G and inset). In the brainstem nuclei, colocalization of Nogo-A and Gpr50 could be detected in the mesencephalic trigeminal nucleus only (Figure 5H). At E18, colocalization of Gpr50 and Nogo-A was detected in the forebrain (Figure 6A), in the cortex at several levels (Figure 6B, C), and in the medullary hindbrain (Figure 6D).

Colocalization of Gpr50 and Abca2 in the adult mouse brain was detected in several areas, including in the ventral third ventricular ependyma (Figure 7A–C, insets) and the lateral side of the epithelium (Figure 7B, inset). In the piriform and

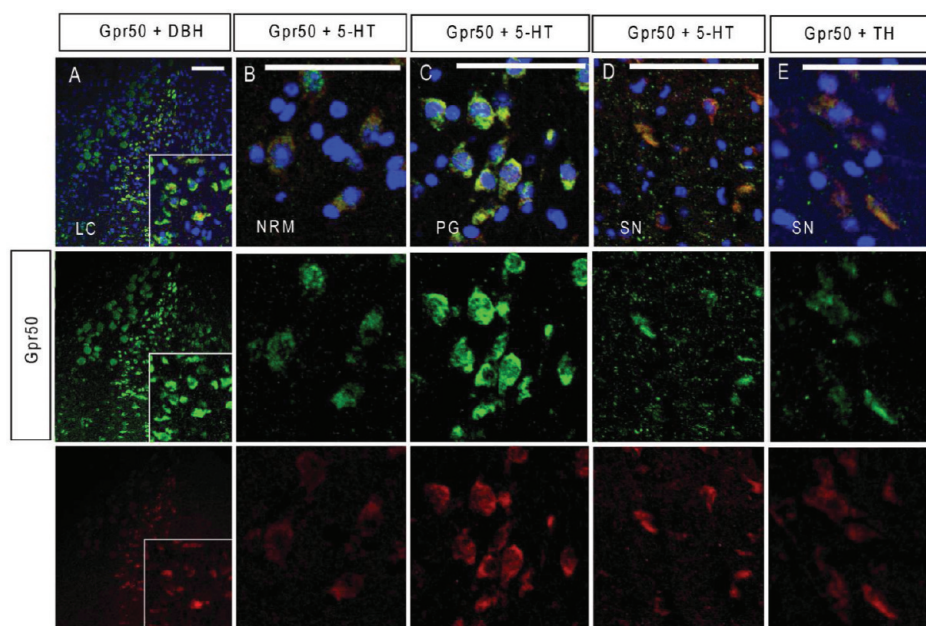


**Figure 4.** Gpr50 colocalizes with noradrenergic, serotonergic, and dopaminergic markers. Adult mouse brains were fixed in 70% EtOH and stained for Gpr50 with dopamine beta hydroxylase (A), 5-HT (B–D), and tyrosine hydroxylase (E). LC = locus coeruleus, NRM = nucleus raphe magnus, PG = pontine gray, SN = substantia nigra. Sections were counterstained with DAPI. Scale bars: 100  $\mu$ m.

somatosensory cortices, colocalization of Gpr50 and Abca2 is widespread (Figure 7D, E), as is colocalization in the brain stem nuclei of the medulla and pons, the parvocellular reticular nucleus (PARN), gigantocellular reticular nucleus (GRN), the principal sensory nucleus of the trigeminal (PSV), and nucleus raphe magnus (NRM) (Figure 7F, inset, G–J). Weak colocalization between Gpr50 and Abca2 was found in the locus coeruleus (LC) and mesencephalic trigeminal nucleus (Me5) (Figure 7I). As indicated by the rt-PCR results, Abca2 expression is much lower in the embryonic brain than in the adult brain and no clear Abca2 staining could be detected at E18.

The Cdh8 antibody detected weak expression in the adult mouse brain (Figure 8A–C). Here Gpr50 and Cdh8 appear to be expressed in a different subset of cells in the median eminence (Figure 8A) but are colocalizing in the periventricular hypothalamus (Figure 8B) and in the amygdala (Figure 8C). Cdh8 is also expressed in the mesencephalic trigeminal nucleus (Figure 8D). In the embryonic brain, Cdh8 expression is stronger and Gpr50 and Cdh8 colocalize in the dorsal forebrain (Figure 9A), the median eminence, and third ventricular epithelium (Figure 9B). Colocalization is also found in the cortex (Figure 9C) and roof plate of the pontine/medullary hindbrain (Figure 9D). Colocalization between Gpr50 and Nogo-A, Cdh8, and Abca2 in the E18 and adult female mouse brain by immunohistochemistry is summarized in Table 1.

Gpr50, Nogo-A, Cdh8, and Abca2 are coexpressed in several hypothalamic (subparaventricular, dorsomedial, and arcuate nuclei) and brain stem nuclei in the pons and medulla (PARN, MARN, PSV, raphe nuclei) involved in the circadian and autonomic regulation of feeding.<sup>32</sup> Gpr50, Nogo-A, Cdh8, and Abca2 were detected in the mesencephalic trigeminal nucleus, a sensory ganglion containing primary sensory neurons involved in the control of automatic (unconscious) activities of food intake such as biting, chewing, and swallowing. Gpr50 was also recently detected in the area prostruma in the medulla,<sup>11</sup> an area associated with nausea and vomiting. These links to

autonomic feeding mechanisms are interesting as *Gpr50* knockout mice appear to show increased energy metabolism, with attenuated weight gain and reduced body fat on a high-energy diet compared to wild-type animals.<sup>10</sup> An intronic SNP in GPR50 was also associated with higher serum triglyceride and lower HDL cholesterol levels.<sup>9</sup> Through homology with the HDL-cholesterol transporter Abca1, Abca2 has also been implicated in lipid metabolism,<sup>33</sup> and knockout mice have an abnormal neurological phenotype that suggests improper regulation of myelin precursors<sup>19</sup> and/or sphingolipids.<sup>34</sup>

The subparaventricular zone and several medullary nuclei including the LC are known to be involved in circadian control of body temperature. Expression of GPR50 in these areas is in agreement with a recently reported role for GPR50 in adaptive thermoregulation and torpor.<sup>11</sup>

Gpr50, Abca2, and Cdh8 expression in the third ventricular ependyma, median eminence, and pars tuberalis may indicate a role in transport of lipids from the CSF/hypothalamus to the portal blood.

Coexpression Gpr50 and interactors in the amygdala may indicate a combined role in fear conditioning and emotional memory<sup>35</sup> and reward learning.<sup>36</sup> GPR50 has been shown to interact with TIP60 and to modulate glucocorticoid receptor signaling,<sup>37</sup> and Gpr50-null mice show altered corticosterone levels,<sup>10</sup> suggesting functions in the regulation of the HPA axis and stress response.

A correlation of *Gpr50* and *Cdh8* expression in prenatal development is interesting as Cadherin 8 is thought to play a role in subdivisional organization of the developing brain.<sup>38–40</sup> Cdh8 expression is implicated in the formation of functional neural circuits involving basal ganglia-thalamocortical<sup>41,42</sup> or fasciculus retroflexus/habenulo-interpeduncular tract.<sup>43</sup> We found *Cdh8* to be expressed in a caudal to rostral peak in the E18 and P7 mouse brain and *Gpr50* was also high in caudal areas at E18. This may indicate a combined role of Cdh8 and Gpr50 in the development of these areas. Gene ontology

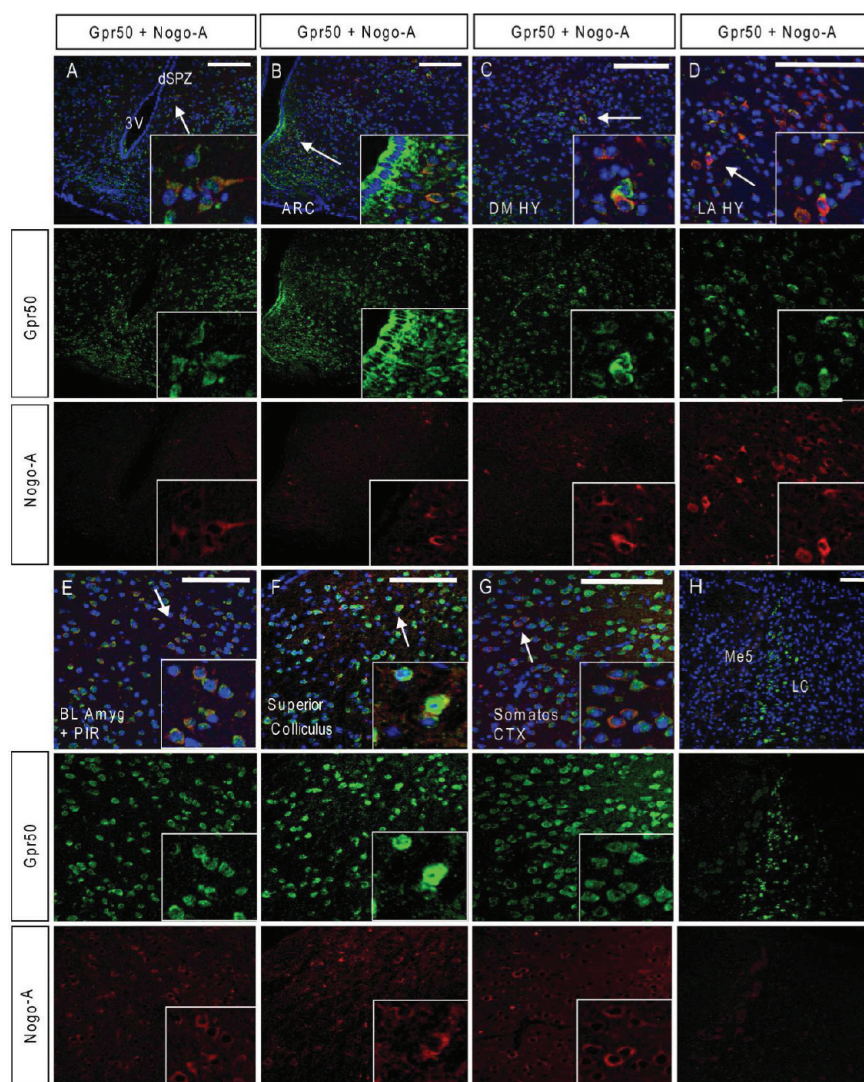


**Figure 5.** Colabeling of Gpr50 with Nogo-A in the adult mouse hypothalamus. Adult CD1 brains were fixed in Methacarn or 70% EtOH stained with Gpr50 and Nogo-A (A–H). dSPZ = dorsal subparaventricular zone, ARC = arcuate nucleus, DM HY = dorsomedial hypothalamus, LA HY = lateral hypothalamus, 3V = third ventricle, BL Amyg = basolateral amygdala, Somatos CTX = somatosensory cortex, LC = locus coeruleus, Me5 = mesencephalic trigeminal nucleus. Scale bars: 100  $\mu\text{m}$ .

analysis of the GPR50 yeast two-hybrid interactors also indicated neural development as a key process.<sup>8</sup>

Investigating the interactions between the HPA axis and the monoaminergic neurotransmitter systems may be key to understanding mental illness.<sup>44</sup> Gpr50 was found to be highly expressed in the hypothalamus and by noradrenergic neurons in the LC. The neurons in the LC have many afferent and efferent connections often modulated by stress.<sup>45</sup> The LC has previously been used as a model system for stress, bipolar disorder, depression, and Alzheimer's disease.<sup>46–48</sup> In order to find out more about the function of GPR50, its function in these brain circuits must be elucidated and the LC may be a good system in which to study this.

The GPR50 genetic association with bipolar disorder was found only in women,<sup>3,4</sup> for reasons yet unclear. Previous studies on Gpr50 expression and behavior have either used males only<sup>10,11,16,24</sup> or have not noted the sex of the animals,<sup>14</sup> possibly explaining some of the differences in expression patterns reported. Moreover, by using males, only sex-specific

behaviors relevant to mental illness may be missed as women are more vulnerable to stress-related psychiatric disorders, such as PTSD and major depressive disorder.<sup>49</sup>

The locus coeruleus may play a role in this, as it is a sexually dimorphic nucleus. It develops over a longer period and is generally larger in female rats.<sup>50,51</sup> Swim stress-induced activation of LC neurons was greater in female rats than in male rats<sup>52</sup> and was related to differential sensitivity of neurons to corticotrophin releasing hormone (CRH) postsynaptically. Sex-specific effects on other parts of the stress response are also significant. Women have higher cortisol levels, and the endocrine responses are possibly more complex with oxytocin and female sex hormones influencing the HPA axis, ACTH, CRH and cortisol levels during the oestrus cycle, breastfeeding, and parturition.<sup>44,53</sup> Although we did not investigate both sexes, our finding of Gpr50 expression in the sexually dimorphic LC and in the stress-associated HPA axis in female mice might provide clues to its functioning and it may be worthwhile to take sex differences into consideration in future (functional) studies of GPR50.

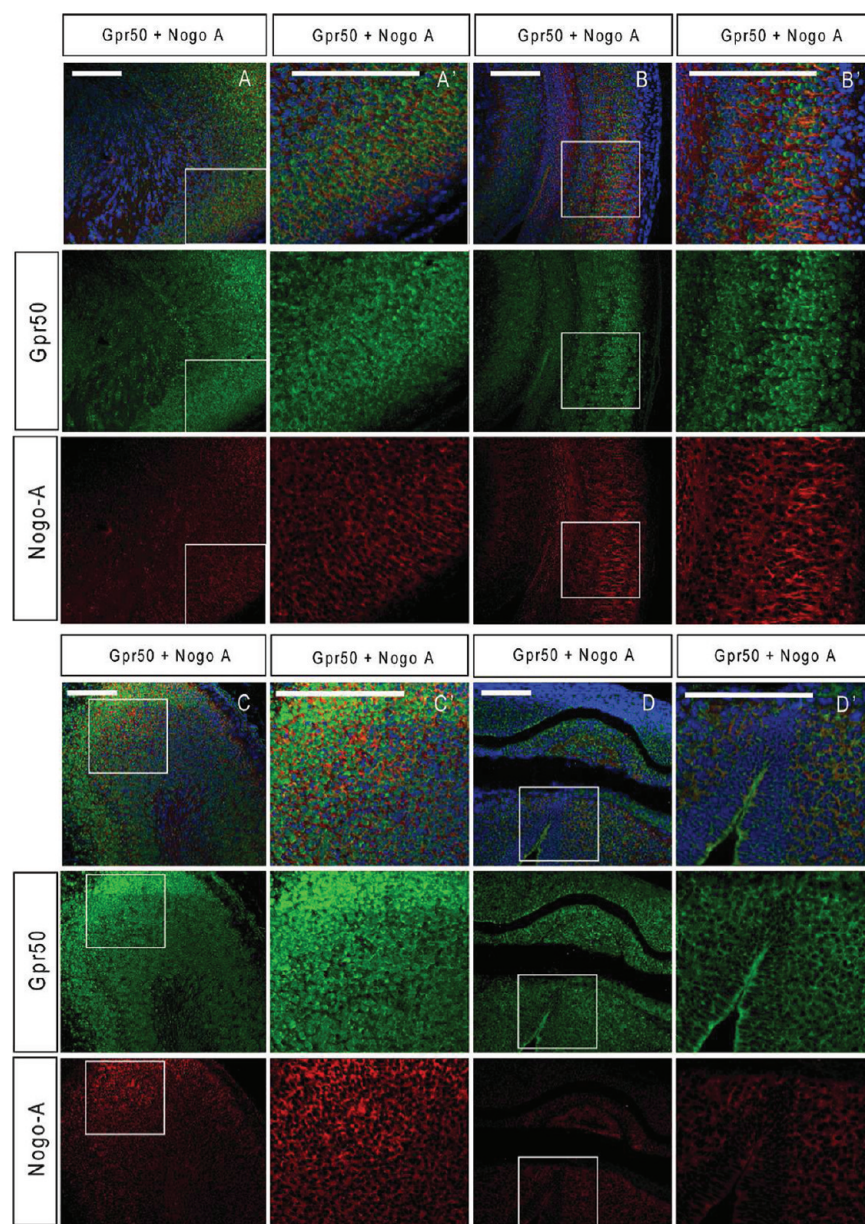


**Figure 6.** Colabeling of Gpr50 with Nogo-A in the E18 mouse brain. E18 CD1 brains were fixed in Methacarn and stained with Gpr50 and Nogo-A (A–D with A'–D' enlargements). (A, A') Dorsal forebrain, (B, B') frontal cortex, (C, C') midbrain cortex, (D, D') medullary hindbrain. Sections are counterstained with DAPI. Scale bars: 100  $\mu$ m.

## SUMMARY

This is the first study investigating the developmental expression of orphan GPR50 receptor. Expression is detected at E13 and peaks at E18, a developmental stage important for axon growth and guidance and synapse formation and function.<sup>54</sup> In addition, we identified many novel sites of Gpr50 expression in the adult and E18 mouse brain, in neurons in the cortex, midbrain, pons, amygdala, and in several brainstem nuclei. We have also identified potential regions of interaction between Gpr50 and Nogo-A, Cdh8, and Abca2. The regions of expression suggest an involvement in neurotransmitter signaling and in particular energy metabolism, thermoregulation, and stress responses, which is consistent with previous studies of Gpr50 expression and function. These areas of expression may provide insight into the link between alteration of GPR50 function and risk of mental illness.

## METHODS

**Antibodies.** Rabbit polyclonal antiserum CDH8 E61 was raised against sequence derived C-terminal peptide residues 785–799: RLGELYSVGESDKET of human CDH8. Final bleeds from immunized rabbits were affinity-purified against both peptides by Eurogentec (Double XP program), and these purified antisera were used in all experiments. We have previously shown that anti-GPR50 (Santa Cruz, CA, sc-50590) specifically binds overexpressed and endogenous GPR50 in cultured mouse neurons and mouse brain fractions (Grünewald et al., 2009). Immunocytochemistry showed predominant expression in the cell membrane, and Western blotting indicated a monomeric species at 67 kDa but also dimers and oligomers as in ref 8. Others have shown staining of Gpr50 in tanycytes lining the third ventricle in mice using this antibody.<sup>11</sup> We also used a GPR50 blocking peptide (Santa Cruz, SC50590-P). Anti-Nogo-A (Santa Cruz, sc-25660) specifically detects endogenous and overexpressed Nogo-A in the ER and plasma membrane in cultured mouse neurons and detects a band at 200 kDa in mouse brain fractions and HEK293 cell



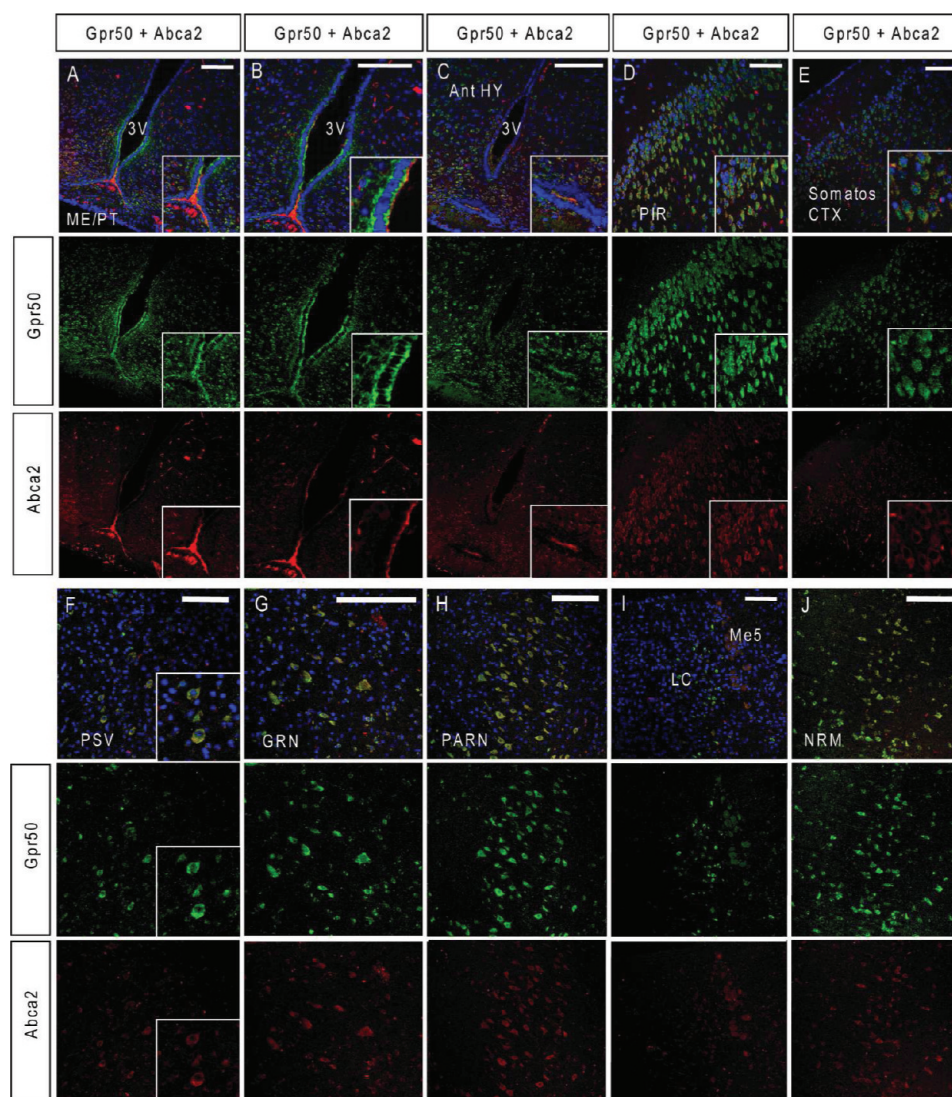


**Figure 7.** Colabeling of Gpr50 with Abca2 in the adult mouse brain. Adult CD1 brains were fixed in Methacarn or 70% EtOH and sections were stained with Gpr50 and Abca2 (A–J). ME = median eminence, PT = pars tuberalis Ant HY = anterior hypothalamus, 3V = third ventricle, PIR = piriform cortex, Somatos CTX = somatosensory cortex, PSV = principal sensory nucleus of the trigeminal, GRN = gigantocellular reticular nucleus, PARN = parvicellular reticular nucleus, LC = locus coeruleus, Me5 = mesencephalic trigeminal nucleus, NRM = nucleus raphe magnus. Nuclei were counterstained with DAPI. Scale bars: 100  $\mu$ m.

lysates.<sup>8</sup> ABCA2 was first characterized in ref 55 and specifically detects ABCA2 by Western blotting at 270 kDa and was shown to localize to punctate intracellular vesicles/lysosomes by immunocytochemistry.

A number of antibodies were used to confirm cell types and used as cell markers: mouse anti-EEA1 (BD transduction laboratories, San Jose, CA, 610457), mouse monoclonal anti-LAMP1 (Abcam, Cambridge MA, ab25630), mouse monoclonal anti-Pan-cadherin (Abcam, ab6528), mouse monoclonal anti-neuronal marker NeuN (Abcam, ab77315), mouse monoclonal against astrocyte marker GFAP (Sigma, St. Louis, MO, G3893), mouse monoclonal against oligodendrocyte marker O4 (R&D systems, Abingdon, U.K., MAB1326), mouse monoclonal against tyrosine hydroxylase (Abcam, ab111), rabbit polyclonal anti-dopamine beta-hydroxylase (DBH) (Abcam, ab43868), and rabbit polyclonal anti-5-HT (Immunostar, Hudson, WI, 20080). Synaptic localization was confirmed using mouse monoclonal anti-PSD-95 (ABR, Golden, CO, MA1-046), mouse monoclonal anti-synaptophysin (Sigma, S5768), and rabbit polyclonal anti- $\alpha$ -tubulin (Abcam, ab4074).

**Mammalian Cell Culture and Transfection.** SH-SY5Y and HEK293T cells were cultured in Dulbecco's modified Eagle's medium

(DMEM; Invitrogen, Paisley, U.K.) with 10% fetal bovine serum (FBS). Cultures were kept at 37 °C with constant humidity, 95% air, and 5% CO<sub>2</sub>. For transient transfections, lipofectamine 2000 was used according to the manufacturer's instructions (Invitrogen).

**Immunocytochemistry.** SHSY-5Y neuroblastoma cells were seeded at  $1 \times 10^5$  on glass coverslips in 12-well dishes and transfected the following day. Cells were transfected with untagged full-length GPR50 (GI:73909216, IOH63602 in pDEST40, Invitrogen), CDH8 (GI:16306538, IOH42822 in pDEST40), and ABCA2.<sup>55</sup> One day after transfection, cells were fixed by incubation with ice cold 100% methanol. Cells were washed with PBS containing 0.2% bovine serum albumin (BSA, Sigma-Aldrich) and blocked for 30 min in PBS/BSA with 10% serum from secondary antibody host. The following primary antibodies in PBS/BSA were incubated for 1 h at room temperature: anti-GPR50 (1:1000), anti-CDH8 E61 (1:1000), anti-ABCA2 (1:1000), anti-EEA1 (1:200), anti-LAMP1 (1:500), and anti-Pan-cadherin (1:1000). Secondary antibodies Alexafluor 594-conjugated donkey anti-rabbit (1:800), 647 chicken anti-mouse (1:500), and 488 donkey anti-goat (1:500) (Molecular probes) were applied for 1 h at room temperature. Glass coverslips were mounted onto slides using a drop of mowiol (Sigma-Aldrich) with DAPI (Vectashield, Vector

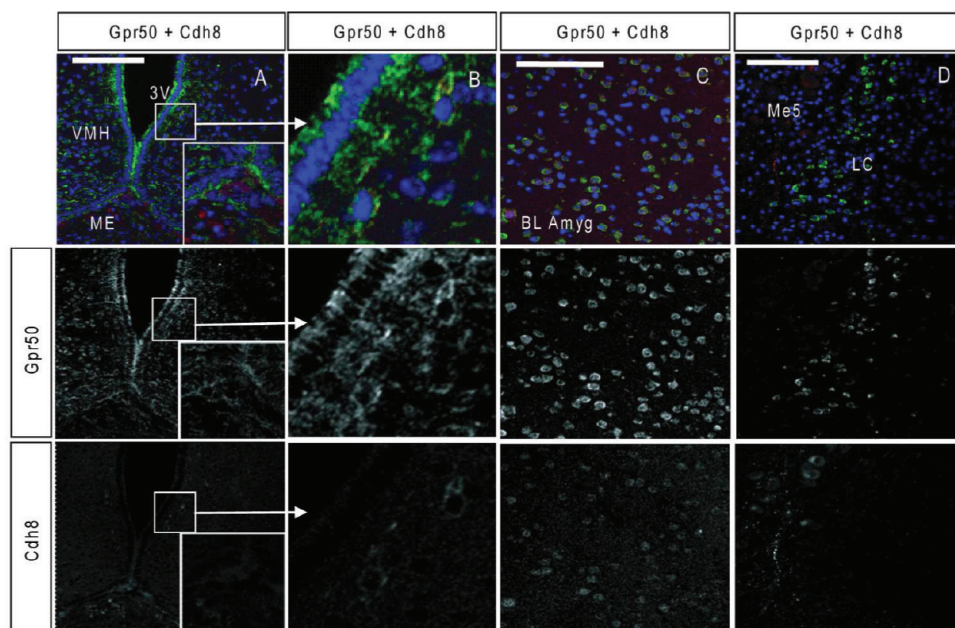


**Figure 8.** Colabeling of Gpr50 with Cdh8 in the adult mouse brain. Adult CD1 brains were fixed in Methacarn or 70% EtOH and stained with Gpr50 (green) and Cdh8 (red) (A–D). VMH = ventromedial hypothalamus, ME = median eminence, 3V = third ventricle, BL Amyg = basolateral amygdala, Me5 = mesencephalic trigeminal nucleus, LC = locus coeruleus. Nuclei were counterstained with DAPI. Scale bars: 100  $\mu$ m.

Laboratories, Peterborough, U.K., 2  $\mu$ g/mL). Secondary antibody controls showed no cross-reactivity between antibodies and nominal background staining.

**Co-immunoprecipitations.** HEK293T cells were grown on 10 cm dishes until 95% confluent and then transfected as above. Twenty-four hours after initiation of transfection, cells were lysed using RIPA buffer (50 mM Tris pH 7.4, 150 mM NaCl, 1% NP-40, 0.1% SDS, 0.5% sodium deoxycholate, plus protease inhibitors (Complete, Roche)). Lysates were incubated on a rotary wheel for 30 min at 4  $^{\circ}$ C, and subsequently cleared from insoluble material at 13,000 rpm at 4  $^{\circ}$ C. The supernatant was incubated for 2 h with 3  $\mu$ g of anti-GPR50. Protein G-sepharose beads (Sigma) were added to the lysate and incubated for 90 min. Beads were collected by centrifugation for 3 min at 10 000 rpm and washed three times with RIPA (all at 4  $^{\circ}$ C). The beads were resuspended in Laemmli sample buffer with 100 mM DTT and boiled for 5 min. The supernatants were analyzed by Western Blotting. PVDF membranes were incubated overnight at 4  $^{\circ}$ C with the following primary antibodies in PBS-Tween20 with 5% milk: anti-ABCA2 (1:1000) and anti-CDH8 (1:3000). Membranes were incubated with a swine anti-rabbit horseradish peroxidase conjugated secondary antibody (1:3000; DAKO A/S, Glostrup, Denmark). Proteins were detected using chemiluminescence (ECL-Plus, Amersham Biosciences, GE healthcare, Chalfont St. Giles, U.K.) and exposure to X-ray film.

**Subcellular Fractionation and Western Blotting.** Ten 7–10 week old female C57BL/6 mice were purchased from Harlan (U.K.). Mice were sacrificed by cervical dislocation and brains were processed for subcellular fractionation and purification of synaptic fractions as described previously.<sup>8</sup> The fractions were analyzed by immunoblotting with anti-CDH8 E61 (1:3000), anti-ABCA2 (1:1000), anti-GPR50 (1:5000), anti-PSD-95 (1:2000), anti-synaptophysin (1:10,000), and anti- $\alpha$ -tubulin (1:200,000). Rabbit anti-mouse (1:2000), rabbit anti-goat (1:5000), and swine anti-rabbit (1:3000) horseradish peroxidase conjugated secondary antibodies (DAKO) were used, and membranes were treated as above. This experiment was performed with three independent samples (30 mice total).

**Real-Time Reverse Transcription Polymerase Chain Reaction (rt-PCR).** The TissueScan Real-Time mouse developmental cDNA panel, consisting of different brain regions at E13, E15, E18, P7, and adult week 5 (total 48 samples) was purchased from Origene Technologies Inc. (lot no.11/06, Rockville, MD). The first strand

cDNAs were synthesized from poly-A<sup>+</sup> RNA using oligo(dT) primers and were normalized to  $\beta$ -actin. The cDNAs were supplied lyophilized and were transported frozen.

Real-time PCR using SYBR Green Supermix (100 mM KCl; 40 mM Tris-HCl, pH 8.4; 0.4 mM of each dNTP; iTaq, DNA polymerase, 50 units/mL; 6 mM MgCl<sub>2</sub>; SYBR Green I; 20 nM fluorescein, and stabilizers; Bio-Rad Inc., Hercules, CA) was performed on the BioRad iCycler. Primers (Supporting Information Table 1) were designed using Primer3 software (<http://primer3.sourceforge.net/>), except for  $\beta$ -actin, which was supplied by Origene. The linear range, correlation coefficient, and PCR efficiency of each primer were determined by producing standard curves in the Biorad iCycler, using mouse brain cDNA as template. Reactions were performed in duplicate. Amplification was achieved in 35 cycles consisting of denaturation at 95  $^{\circ}$ C for 30 s; annealing at 63–65  $^{\circ}$ C for 30 s; and extension at 72  $^{\circ}$ C for 30 s. A melting curve was obtained starting at 55  $^{\circ}$ C with 10 s increments of 0.5  $^{\circ}$ C for 80 cycles. Each PCR reaction generated a single amplicon as indicated by the melting temperature profiles. All PCR products were also checked by gel electrophoresis to confirm correct PCR product size against a 1 kb ladder.

For analysis, the fluorescence threshold value Ct (the number of cycles required for the fluorescent signal to cross the threshold (ie exceeds background level) of each sample was calculated using the iCycler MyiQ system software (Biorad). The relative expression of the genes was determined using the deltaCt method, which generates raw (not normalized) data, relative to the sample with the highest expression. The data are further normalized using a method described by Vandesompele et al.,<sup>56</sup> which is equivalent to using the delta-deltaCt method. It can be performed using the freely available geNorm software: (<http://medgen.ugent.be/~jvdesomp/genorm/>)

Normalized expression data were obtained by dividing the raw gene-of-interest quantities for each sample by the normalization factors, which are the geometric means of the reference genes used in this study:  $\beta$ -actin, Tbp, Hmbs, and cyclophilin B. Spearman correlations ( $r$ , 95% confidence interval), significance at  $p \leq 0.05$ ) were performed using Graphpad Prism.

**Immunohistochemistry.** Female CD1 mice of approximately 10 weeks old were housed in groups of between 5 and 14 animals, depending on cage size. Mice were kept on a 12 h light/dark cycle with lights on at 7.00 h and were fed on SDS RM1 expanded diet with water available ad libitum. Females were taken to the male cage and

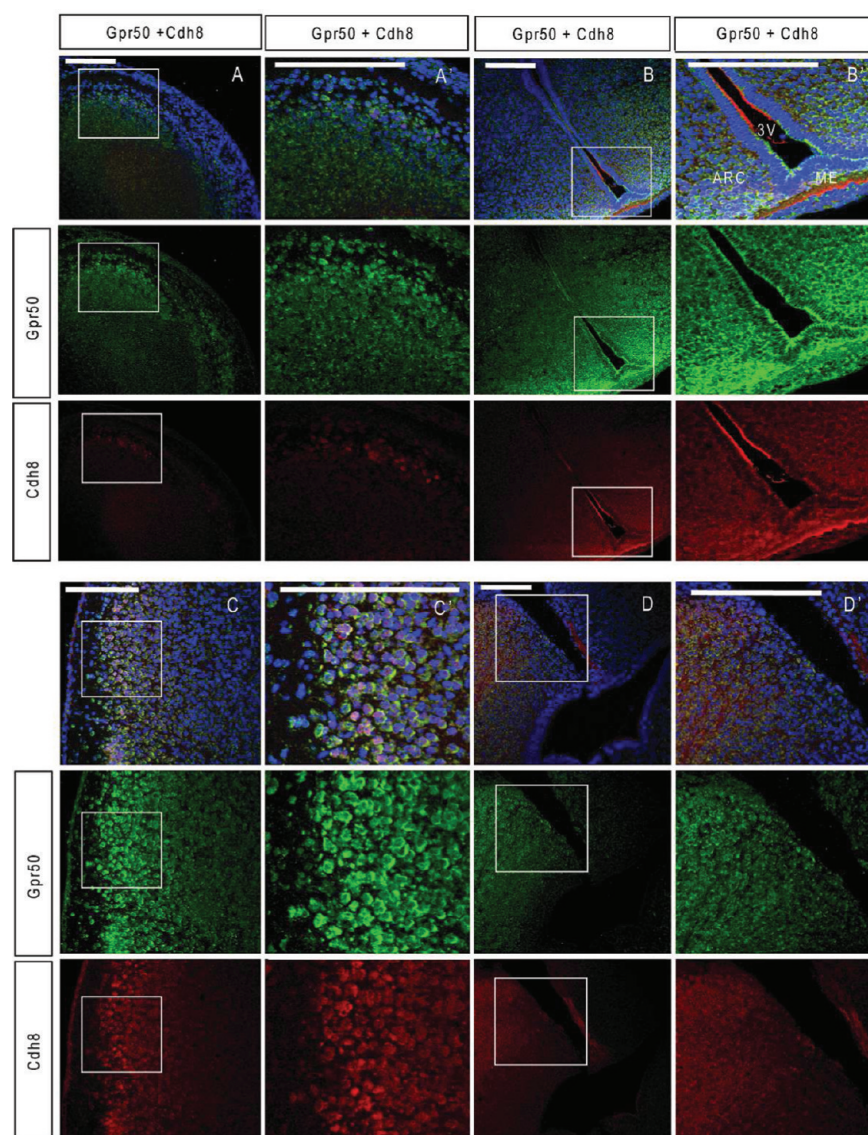


**Figure 9.** Colabeling of Gpr50 with Cdh8 in the E18 mouse brain. E18 CD1 brains were fixed in Methacarn and stained with Gpr50 and Cdh8 (A–D with A'–D' enlargements). A, A': Dorsal forebrain, B, B': hypothalamus and third ventricle, C, C': cortex, D, D': roofplate of the pontine/medullary hindbrain. 3V = third ventricle, ARC = arcuate nucleus, ME = median eminence. Sections are counterstained with DAPI. Scale bars: 100  $\mu$ m.

left until a vaginal plug was found. The female was then housed with other females that were plugged on the same date. The date of the plug was E0. Adult animals were killed by cervical dislocation. Embryos were removed by hysterectomy and brains were directly transferred to ice cold PBS prior to fixation. Three adult female mice and three embryonic day 18 mice were used in this study. Brains were fixed by immersion in 70% ethanol, 10% neutral buffered formalin (3.7% formaldehyde) or Methacarn (60% methanol, 30% chloroform, 10% glacial acetic acid). We found that fixation in 70% ethanol or Methacarn resulted in improved immunoreactivity and cell morphology compared to 4% formaldehyde or 10% formalin. E18 brains were fixed for 4 h at room temperature and adult brains for 16–18 h at 4 °C. Brains were then transferred to 70% ethanol and stored at –20 °C until further processing. Brains were embedded in paraffin wax and cut into 6  $\mu$ m sections on a Leica microtome onto gelatin coated superfrost plus slides (Thermo Fisher, Waltham, MA). Six coronal sections per animal from three individual 10–13 week old CD1 female and E18 mouse brains were processed for immunofluorescent detection of Gpr50 and interactors. Intact coronal sections corresponding to approximately Bregma –0.655 mm, –1.455 mm, –2.88 mm, –3.58 mm, –4.655 mm, and –5.555 mm were chosen from each animal to cover all brain regions evaluated. After sectioning,

slides were dried at 37 °C overnight. Sections were dewaxed in xylene and rehydrated in 100% and 70% EtOH. Before staining, formalin-fixed sections were incubated in picric acid for 20 min and antigen retrieval was performed by microwave boiling slides in 50 mM borate buffer pH 8.0 for 15 min.<sup>57</sup> For chromogenic detection, sections were incubated in 3% H<sub>2</sub>O<sub>2</sub> (Sigma) for 10 min to quench endogenous peroxidases, followed by three washes with PBS. Sections were loaded into Shandon Sequenza slide racks. Tissues were permeabilized in 0.1% triton X-100 (Sigma) in PBS for 30 min, washed twice in PBS/0.02% BSA, and incubated in 6 M guanidine hydrochloride for 10 min.<sup>58</sup> After washing the slides 3 $\times$  with PBS/BSA, sections were incubated in 10% serum from secondary antibody host in PBS/BSA for 30 min. Slides were incubated with the following primary antibodies in PBS for 16–18 h: GPR50 (1:50), Nogo-A (1:100), CDH8 E61 (1:100), ABCA2 (1:500), 5-HT (1:250), NeuN (1:1000), GFAP (1:500), O4 (1:500), dopamine beta-hydroxylase (DBH, 1:250), and tyrosine hydroxylase (TH, 1:250). To assess specificity of staining, brain sections were incubated with a mix of GPR50 antibody and GPR50 blocking peptide. GPR50 antibody (4  $\mu$ g/mL) and blocking peptide (16  $\mu$ g/mL) were preincubated for 1 h at room temperature before addition to the slides. In addition, controls whereby the primary antibody is omitted were performed for Gpr50,

Nogo-A, Cdh8, and Abca2 staining. Slides were washed three times with PBS/BSA before and after incubation with secondary antibodies. For chromogenic detection of proteins, biotinylated rabbit anti-goat (DAKO) was used at 1:500 for 30 min followed by ABC Elite (Vector Laboratories) for 30 min. Proteins were visualized by incubation with DAB (Vector Laboratories). After counterstaining in Harris hematoxylin and lithium carbonate, slides were dehydrated in 70% and 100% ethanol and xylene. Coverslips were then mounted onto slides using pertex. For fluorescent detection, slides were incubated for 1 h with donkey anti-goat (Alexafluor 488, Invitrogen) and donkey anti-rabbit (Alexafluor 594) or donkey anti-mouse (594) in PBS/BSA. Coverslips were mounted onto slides using Vectashield w/DAPI (Vector Laboratories).

**Imaging and Semiquantitative Evaluation of Regional Expression.** Confocal images of neurons were captured sequentially (line) on an Olympus Fluoview 1000 (UPlanSApo 10×/0.4, 20×/0.75, or 60×/1.35 (oil) objectives) or Zeiss LSM510 (Plan Neofluar 20×/0.50 or 40×/0.75 and Plan-Apochromat 63×/1.4 (oil) objectives) confocal laser-scanning microscope at image size 1024 × 1024 using Kalman filter mode 3. Bright-field images were taken on an Olympus BX light microscope fitted with 10×, 20×, and 40× objectives. Secondary antibody controls showed no cross-reactivity between antibodies and nominal background staining. Sections were compared to the adult coronal reference atlas of the Allen Brain Atlas: <http://mouse.brain-map.org>. For the visual evaluation of relative expression levels, each brain region was evaluated for DAB and fluorescence staining intensity based on the following scale: ×, not investigated; −, no expression present; +, weak expression; ++, moderate expression; +++, strong expression.

## ■ ASSOCIATED CONTENT

### ■ Supporting Information

Supplementary Figure 1 containing antibody control experiments, Supplementary Figure 2 containing GPR50 DAB chromogenic and fluorescent images, and Supplementary Table 1 containing details of primers. This material is available free of charge via the Internet at <http://pubs.acs.org>.

## ■ AUTHOR INFORMATION

### Corresponding Author

\*E-mail: Pippa.Thomson@ed.ac.uk.

### Author Contributions

E.G. and P.A.T. designed the experiments. E.G. performed the experiments. K.D.T. provided reagents. E.G., P.A.T., and D.J.P. wrote the manuscript.

### Funding

This work was funded by grants from the MRC (G0401041) and RCUK (EP/E500145/1). E.G. was funded by a Ph.D. studentship of The University of Edinburgh.

### Notes

The authors declare no competing financial interest.

## ■ ABBREVIATIONS

5-HT, 5-hydroxytryptamine, serotonin; ABCA2, ATP-binding cassette subfamily A member 2; AD, Alzheimer's disease; CDH8, Cadherin 8; Co-IP, co-immunoprecipitation; DBH, dopamine beta hydroxylase; DG, dentate gyrus; GPR50, G protein-coupled receptor 50; HDL, high density lipoprotein; HPA, hypothalamic-pituitary-adrenal; LC, locus coeruleus; MES, mesencephalic trigeminal nucleus; MARV, magnocellular reticular nucleus; NRM, nucleus raphe magnus; PARN, parvocellular reticular nucleus; PG, Pontine gray; PIR, piriform cortex; PSD, postsynaptic density; PSV, principle sensory nucleus of the trigeminal; PVN, paraventricular nucleus; Rt-PCR, reverse transcriptase polymerase chain reaction; SN,

substantia nigra; TH, tyrosine hydroxylase; Y2H, yeast two-hybrid

## ■ REFERENCES

- (1) WHO. (2001) The World Health Report 2001- Mental Health: New Understanding, New Hope, pp 24–29, World Health Organisation.
- (2) Kinney, D. K., and Matthyse, S. (1978) Genetic transmission of schizophrenia. *Annu. Rev. Med.* 29, 459–473.
- (3) Macintyre, D. J., McGhee, K. A., Maclean, A. W., Afzal, M., Briffa, K., Henry, B., Thomson, P. A., Muir, W. J., and Blackwood, D. H. (2010) Association of GPR50, an X-linked orphan G protein-coupled receptor, and affective disorder in an independent sample of the Scottish population. *Neurosci. Lett.* 475, 169–173.
- (4) Thomson, P. A., Wray, N. R., Thomson, A. M., Dunbar, D. R., Grassie, M. A., Condie, A., Walker, M. T., Smith, D. J., Pulford, D. J., Muir, W., Blackwood, D. H., and Porteous, D. J. (2005) Sex-specific association between bipolar affective disorder in women and GPR50, an X-linked orphan G protein-coupled receptor. *Mol. Psychiatry* 10, 470–478.
- (5) Dufourny, L., Levasseur, A., Migaud, M., Callebaut, I., Pontarotti, P., Malpoux, B., and Monget, P. (2008) GPR50 is the mammalian ortholog of Mel1c: evidence of rapid evolution in mammals. *BMC Evol. Biol.* 8, 105.
- (6) Reppert, S. M., Weaver, D. R., Ebisawa, T., Mahle, C. D., and Kolakowski, L. F., Jr. (1996) Cloning of a melatonin-related receptor from human pituitary. *FEBS Lett.* 386, 219–224.
- (7) Conway, S., Drew, J. E., Mowat, E. S., Barrett, P., Delagrange, P., and Morgan, P. J. (2000) Chimeric melatonin mtl1 and melatonin-related receptors. Identification of domains and residues participating in ligand binding and receptor activation of the melatonin mtl1 receptor. *J. Biol. Chem.* 275, 20602–20609.
- (8) Grünewald, E., Kinnell, H. L., Porteous, D. J., and Thomson, P. A. (2009) GPR50 interacts with neuronal NOGO-A and affects neurite outgrowth. *Mol. Cell. Neurosci.* 42, 363–371.
- (9) Bhattacharyya, S., Luan, J., Challis, B., Keogh, J., Montague, C., Brennand, J., Morten, J., Lowenbeim, S., Jenkins, S., Farooqi, I. S., Wareham, N. J., and O'Rahilly, S. (2006) Sequence variants in the melatonin-related receptor gene (GPR50) associate with circulating triglyceride and HDL levels. *J. Lipid Res.* 47, 761–766.
- (10) Ivanova, E. A., Bechtold, D. A., Dupre, S. M., Brennand, J., Barrett, P., Luckman, S. M., and Loudon, A. S. (2008) Altered metabolism in the melatonin-related receptor (GPR50) knockout mouse. *Am. J. Physiol. Endocrinol. Metab.* 294, E176–182.
- (11) Bechtold, D. A., Sidibe, A., Saer, B. R., Li, J., Hand, L. E., Ivanova, E. A., Darras, V. M., Dam, J., Jockers, R., Luckman, S. M., and Loudon, A. S. (2012) A Role for the Melatonin-Related Receptor GPR50 in Leptin Signaling, Adaptive Thermogenesis, and Torpor. *Curr. Biol.* 22, 70–77.
- (12) Levoe, A., Dam, J., Ayoub, M. A., Guillaume, J. L., Couturier, C., Delagrange, P., and Jockers, R. (2006) The orphan GPR50 receptor specifically inhibits MT1 melatonin receptor function through heterodimerization. *EMBO J.* 25, 3012–3023.
- (13) Reppert, S. M., Perlow, M. J., Ungerleider, L. G., Mishkin, M., Tamarkin, L., Orloff, D. G., Hoffman, H. J., and Klein, D. C. (1981) Effects of damage to the suprachiasmatic area of the anterior hypothalamus on the daily melatonin and cortisol rhythms in the rhesus monkey. *J. Neurosci.* 1, 1414–1425.
- (14) Drew, J. E., Barrett, P., Mercer, J. G., Moar, K. M., Canet, E., Delagrange, P., and Morgan, P. J. (2001) Localization of the melatonin-related receptor in the rodent brain and peripheral tissues. *J. Neuroendocrinol.* 13, 453–458.
- (15) Vassilatis, D. K., Hohmann, J. G., Zeng, H., Li, F., Ranchalis, J. E., Mortrud, M. T., Brown, A., Rodriguez, S. S., Weller, J. R., Wright, A. C., Bergmann, J. E., and Gaitanaris, G. A. (2003) The G protein-coupled receptor repertoires of human and mouse. *Proc. Natl. Acad. Sci. U.S.A.* 100, 4903–4908.
- (16) Barrett, P., Ivanova, E., Graham, E. S., Ross, A. W., Wilson, D., Ple, H., Mercer, J. G., Ebling, F. J., Schuhler, S., Dupre, S. M., Loudon,

- A., and Morgan, P. J. (2006) Photoperiodic regulation of cellular retinol binding protein, CRBP1 [corrected] and nestin in tanycytes of the third ventricle ependymal layer of the Siberian hamster. *J. Endocrinol.* 191, 687–698.
- (17) Halbleib, J. M., and Nelson, W. J. (2006) Cadherins in development: cell adhesion, sorting, and tissue morphogenesis. *Genes Dev.* 20, 3199–3214.
- (18) Davis, W., Jr., Boyd, J. T., Ile, K. E., and Tew, K. D. (2004) Human ATP-binding cassette transporter-2 (ABCA2) positively regulates low-density lipoprotein receptor expression and negatively regulates cholesterol esterification in Chinese hamster ovary cells. *Biochim. Biophys. Acta* 1683, 89–100.
- (19) Mack, J. T., Beljanski, V., Soulika, A. M., Townsend, D. M., Brown, C. B., Davis, W., and Tew, K. D. (2007) "Skittish" Abca2 knockout mice display tremor, hyperactivity, and abnormal myelin ultrastructure in the central nervous system. *Mol. Cell. Biol.* 27, 44–53.
- (20) Chen, M. S., Huber, A. B., van der Haar, M. E., Frank, M., Schnell, L., Spillmann, A. A., Christ, F., and Schwab, M. E. (2000) Nogo-A is a myelin-associated neurite outgrowth inhibitor and an antigen for monoclonal antibody IN-1. *Nature* 403, 434–439.
- (21) Suzuki, S. C., Furue, H., Koga, K., Jiang, N., Nohmi, M., Shimazaki, Y., Katoh-Fukui, Y., Yokoyama, M., Yoshimura, M., and Takeichi, M. (2007) Cadherin-8 is required for the first relay synapses to receive functional inputs from primary sensory afferents for cold sensation. *J. Neurosci.* 27, 3466–3476.
- (22) Berger, T. W., Semple-Rowland, S., and Basset, J. L. (1981) Hippocampal polymorph neurons are the cells of origin for ipsilateral association and commissural afferents to the dentate gyrus. *Brain Res.* 215, 329–336.
- (23) Morris, R. (1991) Immunoperoxidase Staining of Gene Products in Cultured Cells Using Monoclonal Antibodies. *Methods Mol. Biol.* 7, 339–359.
- (24) Sidibe, A., Mullier, A., Chen, P., Baroncini, M., Boutin, J. A., Delagrangé, P., Prevot, V., and Jockers, R. (2010) Expression of the orphan GPR50 protein in rodent and human dorsomedial hypothalamus, tanycytes and median eminence. *J. Pineal Res.* 48, 263–269.
- (25) Coelho, D. J., Sims, D. J., Ruegg, P. J., Minn, I., Muench, A. R., and Mitchell, P. J. (2005) Cell type-specific and sexually dimorphic expression of transcription factor AP-2 in the adult mouse brain. *Neuroscience* 134, 907–919.
- (26) Ishibashi, H., Nakahata, Y., Eto, K., and Nabekura, J. (2009) Excitation of locus coeruleus noradrenergic neurons by thyrotropin-releasing hormone. *J. Physiol.* 587, 5709–5722.
- (27) Batailler, M., Mullier, A., Sidibe, A., Delagrangé, P., Prevot, V., Jockers, R., and Migaud, M. (2011) Neuroanatomical distribution of the orphan GPR50 receptor in adult sheep and rodent brains. *J. Neuroendocrinol.*
- (28) Mingorance-Le Meur, A., Zheng, B., Soriano, E., and del Rio, J. A. (2007) Involvement of the myelin-associated inhibitor Nogo-A in early cortical development and neuronal maturation. *Cereb. Cortex* 17, 2375–2386.
- (29) Shin, J. W., Shim, E. S., Hwang, G. H., Jung, H. S., Park, J. H., and Sohn, N. W. (2006) Cell size-dependent Nogo-A expression in layer V pyramidal neurons of the rat primary somatosensory cortex. *Neurosci. Lett.* 394, 117–120.
- (30) Zhao, L. X., Zhou, C. J., Tanaka, A., Nakata, M., Hirabayashi, T., Amachi, T., Shioda, S., Ueda, K., and Inagaki, N. (2000) Cloning, characterization and tissue distribution of the rat ATP-binding cassette (ABC) transporter ABC2/ABCA2. *Biochem. J.* 350 (Pt 3), 865–872.
- (31) Zhou, C. J., Inagaki, N., Pleasure, S. J., Zhao, L. X., Kikuyama, S., and Shioda, S. (2002) ATP-binding cassette transporter ABCA2 (ABC2) expression in the developing spinal cord and PNS during myelination. *J. Comp. Neurol.* 451, 334–345.
- (32) Ter Horst, G. J., Copray, J. C., Liem, R. S., and Van Willigen, J. D. (1991) Projections from the rostral parvocellular reticular formation to pontine and medullary nuclei in the rat: involvement in autonomic regulation and orofacial motor control. *Neuroscience* 40, 735–758.
- (33) Kaminski, W. E., Piehler, A., Pullmann, K., Porsch-Ozcurumez, M., Duong, C., Bared, G. M., Buchler, C., and Schmitz, G. (2001) Complete coding sequence, promoter region, and genomic structure of the human ABCA2 gene and evidence for sterol-dependent regulation in macrophages. *Biochem. Biophys. Res. Commun.* 281, 249–258.
- (34) Sakai, H., Tanaka, Y., Tanaka, M., Ban, N., Yamada, K., Matsumura, Y., Watanabe, D., Sasaki, M., Kita, T., and Inagaki, N. (2007) ABCA2 deficiency results in abnormal sphingolipid metabolism in mouse brain. *J. Biol. Chem.* 282, 19692–19699.
- (35) Adolphs, R., Tranel, D., Damasio, H., and Damasio, A. R. (1995) Fear and the human amygdala. *J. Neurosci.* 15, 5879–5891.
- (36) Baxter, M. G., and Murray, E. A. (2002) The amygdala and reward. *Nat. Rev. Neurosci.* 3, 563–573.
- (37) Li, J., Hand, L. E., Meng, Q. J., Loudon, A. S., and Bechtold, D. A. (2011) GPR50 interacts with TIP60 to modulate glucocorticoid receptor signalling. *PLoS One* 6, e23725.
- (38) Korematsu, K., and Redies, C. (1997) Restricted expression of cadherin-8 in segmental and functional subdivisions of the embryonic mouse brain. *Dev. Dyn.* 208, 178–189.
- (39) Bekirov, I. H., Needleman, L. A., Zhang, W., and Benson, D. L. (2002) Identification and localization of multiple classic cadherins in developing rat limbic system. *Neuroscience* 115, 213–227.
- (40) Suzuki, S. C., Inoue, T., Kimura, Y., Tanaka, T., and Takeichi, M. (1997) Neuronal circuits are subdivided by differential expression of type-II classic cadherins in postnatal mouse brains. *Mol. Cell. Neurosci.* 9, 433–447.
- (41) Alexander, G. E., and Crutcher, M. D. (1990) Functional architecture of basal ganglia circuits: neural substrates of parallel processing. *Trends Neurosci.* 13, 266–271.
- (42) Korematsu, K., Nishi, T., Okamura, A., Goto, S., Morioka, M., Hamada, J., and Ushio, Y. (1998) Cadherin-8 protein expression in gray matter structures and nerve fibers of the neonatal and adult mouse brain. *Neuroscience* 87, 303–315.
- (43) Marchand, E. R., Riley, J. N., and Moore, R. Y. (1980) Interpeduncular nucleus afferents in the rat. *Brain Res.* 193, 339–352.
- (44) Swaab, D. F., Bao, A. M., and Lucassen, P. J. (2005) The stress system in the human brain in depression and neurodegeneration. *Ageing Res. Rev.* 4, 141–194.
- (45) Cunningham, E. T., Jr., and Sawchenko, P. E. (1988) Anatomical specificity of noradrenergic inputs to the paraventricular and supraoptic nuclei of the rat hypothalamus. *J. Comp. Neurol.* 274, 60–76.
- (46) German, D. C., Manaye, K. F., White, C. L., 3rd, Woodward, D. J., McIntire, D. D., Smith, W. K., Kalaria, R. N., and Mann, D. M. (1992) Disease-specific patterns of locus coeruleus cell loss. *Ann. Neurol.* 32, 667–676.
- (47) Wiste, A. K., Arango, V., Ellis, S. P., Mann, J. J., and Underwood, M. D. (2008) Norepinephrine and serotonin imbalance in the locus coeruleus in bipolar disorder. *Bipolar Disord.* 10, 349–359.
- (48) Zhu, M. Y., Klimek, V., Dilley, G. E., Haycock, J. W., Stockmeier, C., Overholser, J. C., Meltzer, H. Y., and Ordway, G. A. (1999) Elevated levels of tyrosine hydroxylase in the locus coeruleus in major depression. *Biol. Psychiatry* 46, 1275–1286.
- (49) Kuehner, C. (2003) Gender differences in unipolar depression: an update of epidemiological findings and possible explanations. *Acta Psychiatr. Neurol. Scand.* 108, 163–174.
- (50) Luque, J. M., de Blas, M. R., Segovia, S., and Guillamon, A. (1992) Sexual dimorphism of the dopamine-beta-hydroxylase-immunoreactive neurons in the rat locus ceruleus. *Brain Res. Dev. Brain Res.* 67, 211–215.
- (51) Pinos, H., Collado, P., Rodriguez-Zafra, M., Rodriguez, C., Segovia, S., and Guillamon, A. (2001) The development of sex differences in the locus coeruleus of the rat. *Brain Res. Bull.* 56, 73–78.
- (52) Curtis, A. L., Bethea, T., and Valentino, R. J. (2006) Sexually dimorphic responses of the brain norepinephrine system to stress and corticotropin-releasing factor. *Neuropsychopharmacology* 31, 544–554.
- (53) Chiodera, P., Volpi, R., Capretti, L., Marchesi, C., d'Amato, L., De Ferri, A., Bianconi, L., and Coiro, V. (1991) Effect of estrogen or

insulin-induced hypoglycemia on plasma oxytocin levels in bulimia and anorexia nervosa. *Metabolism* 40, 1226–1230.

(54) Matsuki, T., Hori, G., and Furuichi, T. (2005) Gene expression profiling during the embryonic development of mouse brain using an oligonucleotide-based microarray system. *Brain Res.* 136, 231–254.

(55) Vulevic, B., Chen, Z., Boyd, J. T., Davis, W., Jr., Walsh, E. S., Belinsky, M. G., and Tew, K. D. (2001) Cloning and characterization of human adenosine 5'-triphosphate-binding cassette, sub-family A, transporter 2 (ABCA2). *Cancer Res.* 61, 3339–3347.

(56) Vandesompele, J., De Preter, K., Pattyn, F., Poppe, B., Van Roy, N., De Paepe, A., and Speleman, F. (2002) Accurate normalization of real-time quantitative RT-PCR data by geometric averaging of multiple internal control genes. *Genome Biol.* 3, RESEARCH0034.

(57) Yamashita, S. (2007) Heat-induced antigen retrieval: mechanisms and application to histochemistry. *Prog. Histochem. Cytochem.* 41, 141–200.

(58) Peranen, J., Rikkinen, M., and Kaariainen, L. (1993) A method for exposing hidden antigenic sites in paraformaldehyde-fixed cultured cells, applied to initially unreactive antibodies. *J. Histochem. Cytochem.* 41, 447–454.